Search for Lorentz Invariance with flares in Active galactic nuclei

DESY Summer Student Programme, 2014

Alessandra Costantino

Università degli Studi di Bari Aldo Moro, Italiy

Supervisor
Gernot Maier
Anna O'Faolain de Bhroithe

5th of September 2014

Abstract

Some theories of quantum gravity suggest that there might be a violation of Lorentz invariance at high photon energy. The energy size scale of these effects is E_{QG}, generally assumed to be of the order of the Planck mass ($E_P = 10^{19}$ GeV). After producing a toy Monte Carlo simulation to test the analysis procedure, data from a flare in the AGN Mrk421 measured by VERITAS in February 2010 were analyzed in order to constrain the value of E_{QG}. A 95% confidence lower limit of 1.1×10^{11} TeV was obtained from this analysis.

Contents

1 Introduction

Nowadays the description of nature is based on two disconnected pieces, which grew out of the fast development of the scientific knowledge which took place in the 20^{th} century, namely, quantum mechanics and general relativity. Both theories are widely confirmed by experience. The first one laid the foundation for the comprehension of many physical phenomena on the subatomic, atomic and molecular levels. The latter is the basis of the studies involving gravitational phenomena.
These two theories appear both incomplete and in contrast to one another. The main challenge of the 21^{st} century for theoretical Physics is to bring to completion the scientific revolution that began in the past century. The hypothetical theory combining the innovations of quantum mechanics and general relativity, and describing the quantum features of the gravitational phenomena is *quantum gravity* (QG). A possible observable effect of QG is outlined in Section 1.1. This effect is explored using data on the bright and variable blazar Markarian421 (Mrk421) taken with VERITAS. The source is described in Section 1.2 and the instrument and observation are outlined in Section 1.3. A toy Monte Carlo simulation is created to test and calibrate the analysis procedure. This is presented in Section 2. Finally, the results of the data analysis are given in Section 3.

1.1 Quantum gravity phenomenology in the energy dispersion relation

Quantum gravity is needed to understand phenomena which are characterized by very high energies, that is to say very small length scale (of the order of the Planck length $L_p \approx 10^{-35}m$). Analyses of observations of GRBs at sub-MeV energies and later AGN flares at TeV energies have been performed considering Planck-scale effects leading to a departure from classical Lorentz symmetry[4].
Classical Lorentz symmetry is a manifestation of the classical light cone structure in Minkowsky spacetime. Introducing some "quantum features" in spacetime structure may then influence the Lorentz symmetry. The violation of Lorentz invariance could be a testable prediction of theories which are considered as candidates for the solution of the quantum gravity problem. Some of these theories predict that high energy photons have a reduced propagation speed. The magnitude of this phenomenon is set by an assumed energy scale, E_{QG}, according to

$$v = \frac{\partial E}{\partial p} \approx c\left[1 + \xi\frac{E}{E_{QG}} - \mathcal{O}\left(\frac{E}{E_{QG}}\right)^2\right] \tag{1}$$

If we consider a gamma-ray astrophysical source, this time shift of high energy photons will result in a time delay for signals arriving on the Earth from a source at cosmological distance z. The first-order differential time delay is given by

$$\frac{\partial t}{\partial E} \approx \frac{\xi}{H_O E_{QG}}\int_0^z \frac{dz}{h(z)}, \tag{2}$$

where t is the photon arrival time, $h(z) = \sqrt{\Omega_\Lambda + \Omega_M(1+z)^3}$, and $\Omega_\Lambda = 0.71$, $\Omega_M = 0.29$, and $H_0 = 72$ km s^{-1} Mpc^{-1} [4]. Using data from experiments such as VERITAS, it is possible to constrain the Lorentz symmetry breaking term in the dispersion relation.

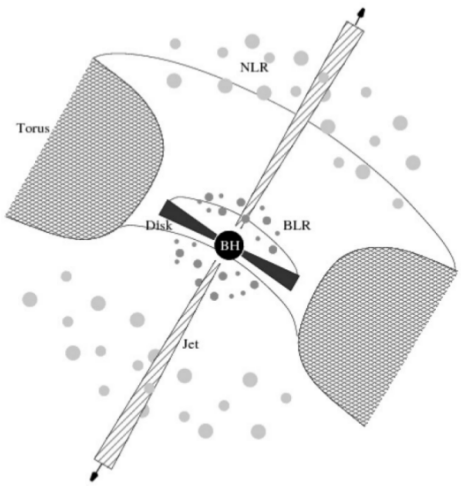

Figure 1: The diagram of the current paradigm of an AGN. Not to scale. Picture taken from [6]

1.2 Markarian 421

Mrk 421 was the first detected extragalactic VHE gamma-ray source (E>10GeV). It was first observed in 1992 at the Fred Lawrence Whipple Observatory in Arizona by the "Whipple 10 m" atmospheric-Cherenkov imaging telescope. It is located at a redshift z=0.031. Its spectrum is represented by a power-law with spectral index $\Gamma = 2.2$, though it has been found to vary and it shows evidence for an exponential cutoff. The most relevant features of Mrk 421 are the remarkable flux variability, correlation with X-rays and intense VHE flaring.
Mrk421 is an example of blazar, a type of active galactic nucleus (AGN). The term AGN refers to the central region of a galaxy which produces more radiation than the entire galaxy. The emission spectrum covers a wide portion of the electromagnetic spectrum from radio to gamma rays. In general, an AGN is composed of the following elements:

- A **Supermassive black hole**, of 10^6 to 10^{10} solar masses is the most likely candidate for the central engine.
- The **accretion disk** is formed by material close to the black hole.
- The **broad-line region**. The gas clouds close to the center are ionized by the thermal radiation coming from the disk. As a result, there is UV/optical light emission from these clouds. The emission lines are broadened due to the Doppler effect, since these clouds move very fast (1000-10000 km/s).
- The slower moving gas clouds (100 km/s) further away from the center form the **narrow-line region**. In this region the absorption/emission of light produces a narrow-line spectrum.
- Along the equatorial line of the source a **dusty torus** is located. It is formed of gas and dust and it obscures the optical and UV radiation from that region. Part of the

radiation emitted by the central region is absorbed by it, and then re-emitted in the infrared region.

- **Jets** are collimated outflows emerging in opposite directions perpendicular to the accretion disk. There are many theoretical models about the composition and the formation mechanisms of these jets, but the resolution of current astronomical instruments does not provide enough information to confirm or reject scenarios. Jets extends from sub- to hundreds of kps, and have different morphologies. Radio observations of AGN jets shows that individual components are higly relativistic (more than 99% the speed of light).

Blazars are active galactic nuclei with the relativistic jets almost aligned with the observer's line of sight. They can remain collimated for hundreds of thousands of light-years. Blazars are characterized by high observed luminosity, rapid variability and apparent superluminal motion of the jets. These features can be explained with the particular jet orientation.
The VHE flux from Mrk 421 is extremely variable in different timescales. Average yearly rates vary between 0.23 and 1.86 Crab units. VHE gamma ray observations showed episodes of flares in which the flux level exceeded 10 Crab units in time bins of less than 5 minutes.
The high flux and fast variability time scale of Mrk421 can be used to probe the extent of Lorentz symmetry breaking that may be present.

1.3 The IACT technique and VERITAS

Air Showers Electromagnetic showers are generated by gamma rays impinging on Earth and interacting with the atmospheric nuclei. When the gamma-ray enters the atmosphere, it pair produces. The electron and the positron produced have a small deviation from the original gamma trajectory and can produce further gamma rays by means of *brehmsstrahlung*. The electron-photon cascade then develops.
The penetration depth of the shower depends on the energy of the primary gamma ray. Typically electromagnetic showers have a longitudinal extension of several kilometers and a width of hundreds of meters. The maximum number of electromagneetic particles in the shower is located at 8-12 km in altitude in the atmosphere in the case of vertical incidence.

The Cherenkov effect A fraction of the electrons and positrons prduced in the electromagnetic shower travel with superluminal speed in the atmosphere and produce Cherenkov photons, mainly in the near UV region of the electromagnetic spectrum. At about 10 km a.s.l. the Cherenkov threshold is around 40 MeV, and the Cherenkov emission angle is less than 0.7 °. Cherenkov light then reaches the ground within a circle of about 150 m in diameter.

IACT The term Imaging Atmospheric Cherenkov Telescopes (IACT) refers to telescopes which can detect VHE gamma-rays in the 50GeV-50TeV range. Cherenkov light emitted during an electromagnetic shower is reflected by the telescope dish onto its focal plane where a multi-pixel camera records the shower image.
The camera consists of hundreds of photodetectors, usually photomultiplier(PMT) tubes. The image of the showers recorded by the camera is approximately elliptical. The number of photons detected depends on the energy of the primary photons, while the orientation of the image in the camera provides information about the direction of the incoming photon.

Energy range	100 GeV to >30 TeV (spectral reconstruction starts at 150 GeV)
Energy resolution	15% at 1 TeV
Angular resolution	0.1 deg at 1 TeV, 0.14 deg at 200 GeV (68% containment radius)
Source location accuracy	50 arcseconds
Point source sensitivity (with new array configuration)	1% Crab in < 30h, 10% in 30 min

Table 1: VERITAS key characteristics [2]

VERITAS VERITAS (Very Energetic Radiation Imaging Telescopes Array System) is a major ground-based gamma-ray observatory. It is located at the base camp of the Fred Lawrence Whipple Observatory in Southern Arizona, 1268 m a.s.l. The array is composed of four telescopes, whose optical diameter is 12 m. Each telescope is provided with a multi pixel PMT camera, with a field of view of $\approx 3.5°$. The key characteristics of VERITAS are shown in Table 1.

2 Monte Carlo simulation

The first part of my job consisted of simulating a typical light curve of a blazar.

- I first reproduced the measured spectrum of this kind of source, which is a power-law

$$\frac{dN}{dE} = N_0 \left(\frac{E}{1TeV}\right)^{-\Gamma} . \tag{3}$$

  The spectral index Γ was first set equal to 2.2, and then varied. The energy range used for the simulation (0.2 TeV- 30 TeV) was chosen to match VERITAS Energy range(Table [1]). Figure 2 shows the simulated energy spectrum.

- Then a typical light curve of the source was drawn. An observation time of 1400 minutes was chosen, and divided into time bins of 4 minutes. Each time bin was filled in with a random number of photons drawn from a Poissonian distribution with average 5. Each photon was then assigned a random energy drawn from the power-law distribution.

- Noise was added to the light curve in order to take into account uncertainties in the background estimation. Each time bin was also filled in with a random number of photons drawn from a poissonian distribution with an average flux of 0.5 photons per minute. The spectrum of the noise was assumed to be the cosmic ray spectrum, with a spectral index of -2.7.

- Several flares of different shapes were added randomly during the whole observation time. The time evolution of the photon flux was assumed to be gaussian, while the energy spectrum was assumed to be also a power-law with spectral index of 2.4. The mean for each gaussian was drawn from a uniform distribution in the whole

observation time interval. The sigma was drawn from a uniform distribution between 10 minutes and 40 minutes. Each time bin was then filled in with a number of photons drawn from a poissonian distribution averaged on the value of the gaussian at that time. The number of flares occurring during the observation time is also randomly chosen form a uniform distribtion. An example of a simulated light curve including noise and flares is shown in figure 3.

- An energy smearing of 15% was introduced to simulate the energy resolution of the telescopes. The energy assigned to each photon was drawn from a gaussian distribution centered on the value randomly drawn from the power-law spectrum.
- To each photon belonging to the source emission, a time delay was assigned according to the dispersion relation, depending on the photon energy. The input value of E_{QG} was $1.8 \cdot 10^{14}$ TeV [4].
- The light curve was divided into several energy bins. The delay of the photons shows itself in the highest energy bins by means of a shift of the flares (see figure 6).

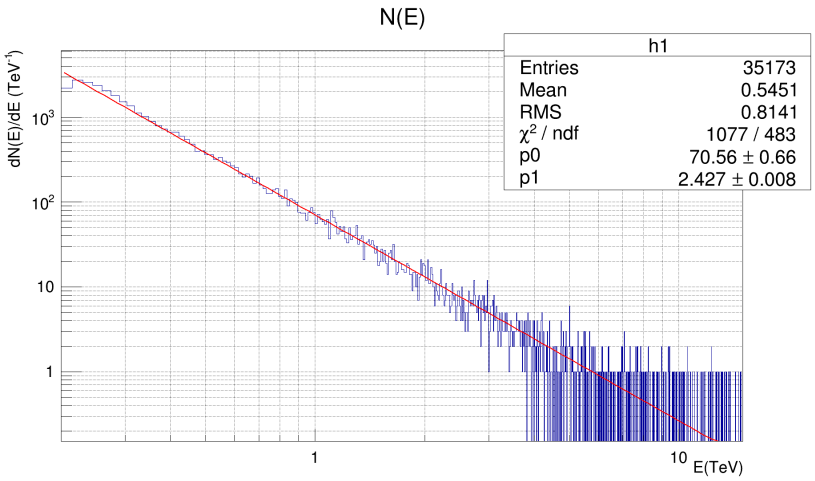

Figure 2: The simulated energy spectrum of the source.

The analysis of the simulation results was then performed. In order to obtain the value of E_{QG} the peaking time of the flare was evaluated in each energy bin by means of a gaussian fit. The peaking time was then plotted against the average of each energy bin, with the aim to verify the dependence of photons arrival time on their energy. The energy value plotted in graph 5 is the average of the energy bin, weighted on the power-law distribution of the events.
A linear fit was then performed and the value of E_{QG} drawn from the first-order equation for differential time delay was evaluated from the slope of the curve.
The value of E_{QG} obtained from the fit is $6 \times 10^{13} \pm 1 \times 10^{13}$ TeV, while the inserted value was 1.8×10^{14}. This discrepancy is expected, and it is due to the fact that the energy of photons in the widest energy bin can be very different one from the other. The peaking time is then overestimated, because the gaussian in the highest energy bin is the superimposition of several gaussians with different means. A calibration curve was also drawn (6) for different values of the spectral index. As the spectral index increases the

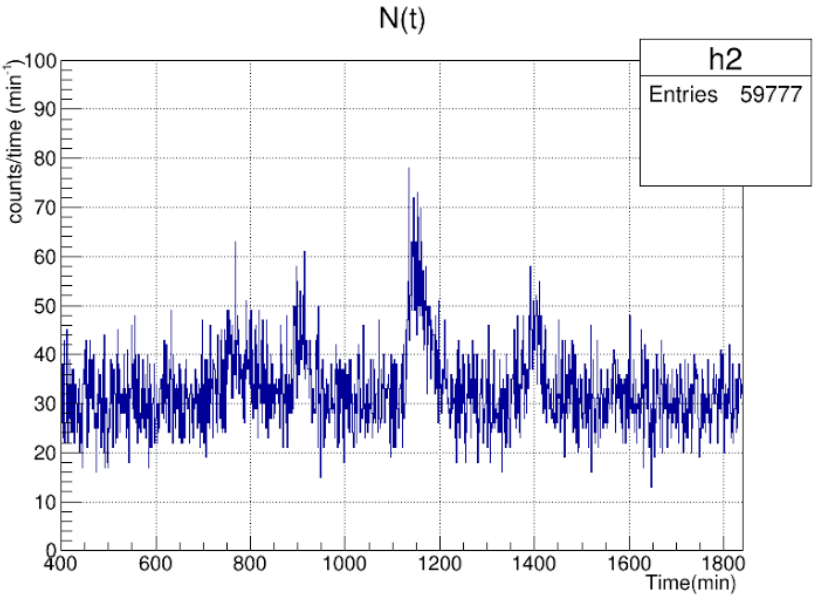

Figure 3: An example of a simulated light curve including background noise, a constant component from the source and random flares superimposed. The width of the time bins is 1 minute.

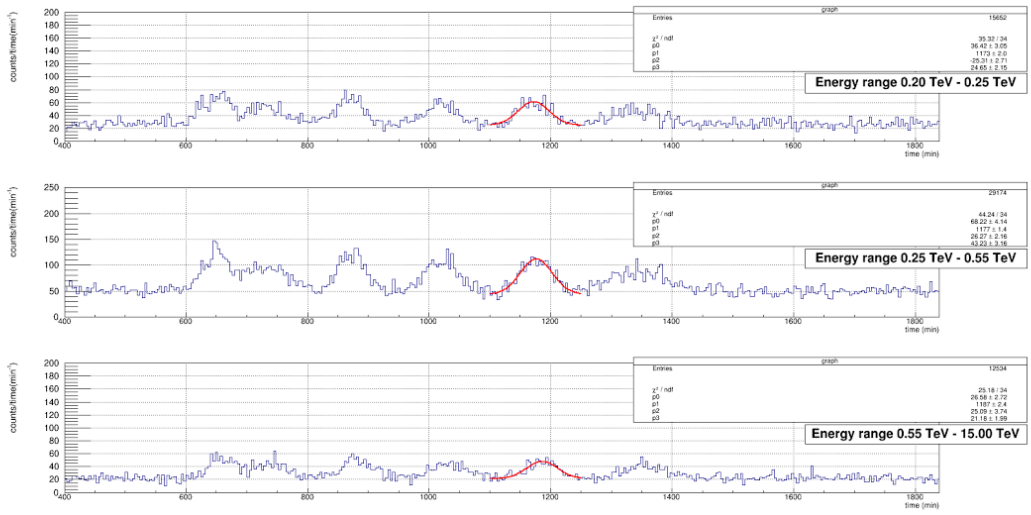

Figure 4: Light curves in different energy bins. The width of the time bins is 4 minutes.

population of the last energy bin decreases, making it difficult to resolve the flare in that bin. This effect is shown in the graph in picture 7.

3 Data analysis and results

The second part of my project consisted of analysing a light curve from Mrk421 in order to test Lorentz Invariance and find a lower limit for the value of E_{QG}. The data I analyzed are from a big flare measured in February 2010. The flux reached up to ≈ 8 Crab units on

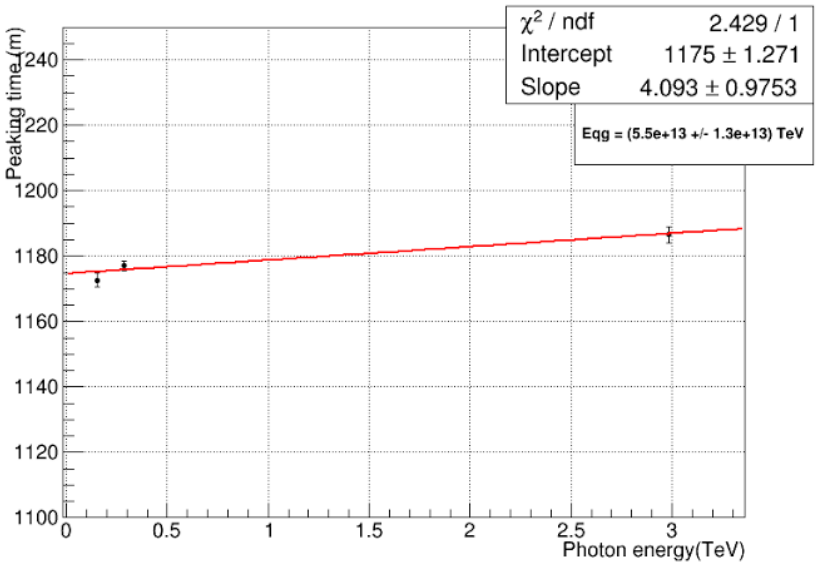

Figure 5: The plot represents the peaking time resulting from the gaussian fit vs the weighted average of the energy bin. The value of E_{QG} resulting from the fit is $6 \times 10^{13} \pm 1 \times 10^{13}$ TeV, while the imput value was 1.8×10^{13}.

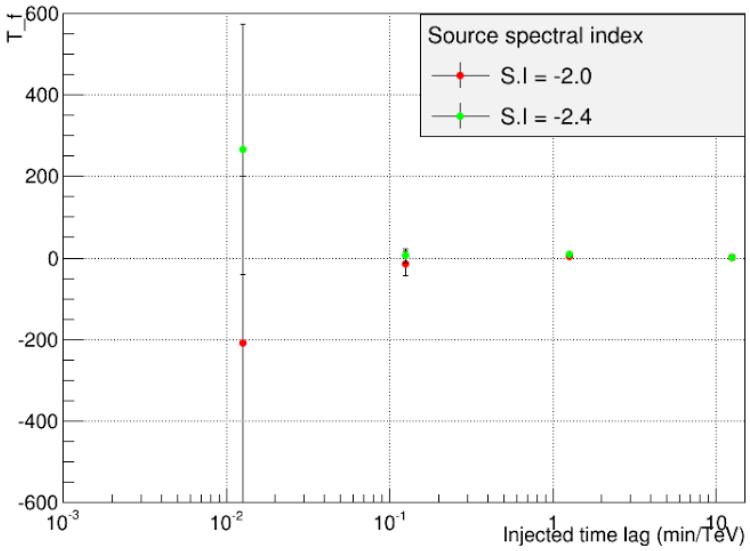

Figure 6: The plot represents the ratio between the fit time lag and the injected time lag divided by the injected time lag.

this night, making it an extremely bright event.
A light curve was produced by means of the software package *eventdisplay*, which performs the parametrization of the image in each camera, the reconstruction of each event and, after separation of photons and hadrons, derives an energy spectrum and a light curve.

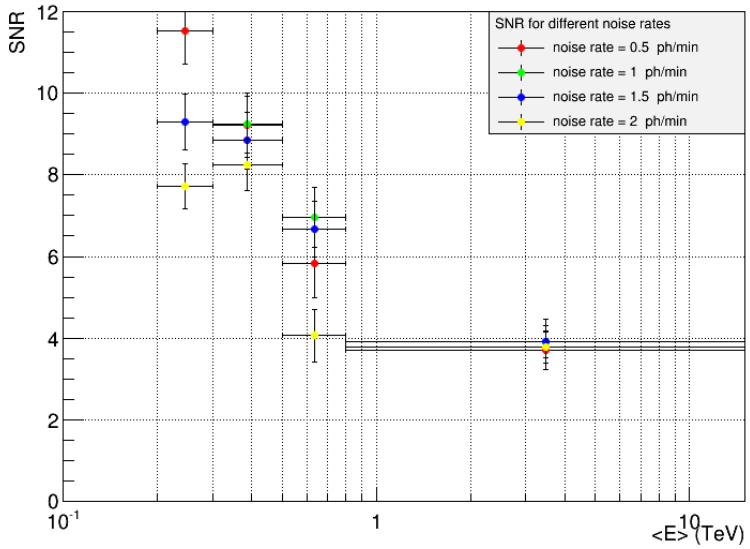

Figure 7: The value of the signal-to noise ratio of the light curve in correspondence to the position of the flare vs the average of each the energy bin for different values of the backgroud noise. As it is possible to notice, the power-law spectum makes it difficult to resolve the flare in the highest energy bins. The noise background rate was evaluated by means of a linear fit in a flat region of the light curve

The first stage of the analysis consists of the conversion of the signal in the PMTs into the value of the charge produced in each pixel. The image in the camera is then reconstructed. The image is then parametrized ([5]) with the aim to reconstruct the event. The parameters evaluated are the *size* of the image, the *width* and the *length*. The size of the image is the sum of the integrated charge of all pixels and is related to the energy of the primary particle. The width and the length relate to the lateral and longitudinal development of the cascade.

The Cherenkov light emitted from a showering particle produces a roughly elliptical image in the Camera. The major axis of the image represents the image of the shower axis. It points towards the image of the source on one side, and to the point where the shower axis intersects the plane of the telescope dish on the other side. The image of the source is obtained by means of the superimposition of the camera images. Then a weighted average of the intersection of all pairs of major axes, taking into account the angle between the two axes, the size and the ratio of width-over-length from each image.[5]
The position of the shower core is then reconstructed. The shower core is the position where the incoming photon would have hit the ground. It is reconstructed by a similar average of the intersection of couples of image axes, starting from the telescope locations, projected on the shower plane (the plane perpendicular to the arrival direction of the shower).
The energy of the incoming photon is proportional to the number of Cherenkov photons emitted during the shower. Therefore the energy is related to the size of the image. The energy of the primary particle is evaluated by means of lookup tables based on MC simulation of the size of the image varying other observation conditions.

Figure 8: The light curve represented. The colored areas represents the peaks. The red marker represents the average evaluated. The plot above represents the light curve for photons of energy 10 GeV<E<34 GeV. The plot below represents the light curve of photons of energy 41 GeV<E 30 TeV

Once the event is reconstructed, shape cuts are applied to eliminate hadronic showers. Since hadronic showers are more irregular, their images are different. The cuts are based on lookup tables of the parameters of the electromagnetic shower. The distribution of the parameters of an hadronic shower image significantly differs from the one expected for an electromegnetic shower.
The isotropic cosmic-ray background is kept under control by means of a cut on the angle on the sky between the assumed source position and the reconstructed shower direction. The remaining background rate is then estimated. This is done by creating a sky-map, which contains the reconstructed shower direction for each gamma-ray-like event. The excess number of events is then calculated subtracting the number of events in a region far off the assumed source position from the number of events in a circular region centered on it.

Effective areas are used to reconstruct the flux from the gamma-ray source. The effective area is an estimate of the efficiency of the instrument to detect gamma photons. Its value is calculeted by means of MC simulations as

$$A_{EFF}(E) \propto \frac{N_{sel}}{N_{sim}}, \tag{4}$$

where N_{sel} is the number of selected events and N_{sim} is the number of simulated events. This parameter is used to evaluate the flux of photons from the source in photons $s^{-1}cm{-}2$.

The integral flux plotted against time is called light curve. It is useful to analyse the temporal evolution of a source, and can be produced with different binnings.
For this analysis a 4-minute binning was chosen. The choice of the binning is related to the necessity to have a significant flux in each bin. On the other hand, too wide time bins would lead to a worse resolution of the flares.

3.1 Results

The energy spectrum of the source is shown in the graph in figure 9 along with the result of the fit performed on the energy spectrum. The fit function is a simple power law.

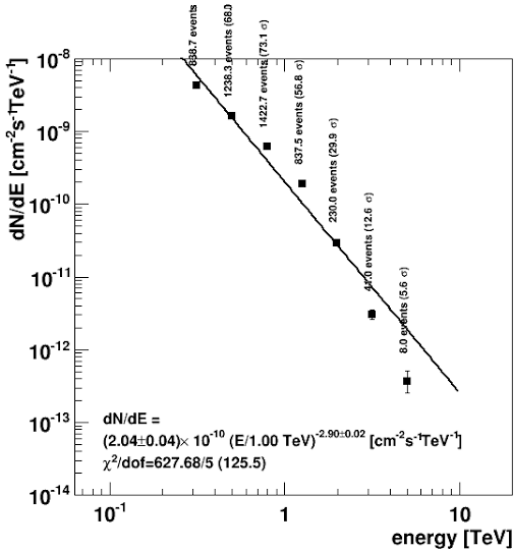

Figure 9: The energy spectrum of Mrk421 evaluated by means of data taken in MJD 55244

$$\phi(E) = \phi_0 \left(\frac{E}{E_0}\right)^{-\Gamma}, \tag{5}$$

Where ϕ_0 is a normalization constant, $E_0 = 1\text{TeV}$ is a normalization energy and Γ is the photon spectral index. The fit values for the parameters of the spectrum are $\phi_0 = 2.04 \pm 0.04 \times 10^{-10}\text{cm}^{-2}\text{s}^{-1}$ TeV^{-1}, $\Gamma = 2.90 \pm 0.02$.
The light curve was produced in two energy bins and is shown in figure 8. A value of energy $\langle E \rangle$ was assigned to each bin by means of a weighted average using the power-law fit to the energy spectrum.
Since the shape of the flares is almost symmetrical and the peaking time T was evaluated by averaging the histogram in a region surrounding each maximum. The error on the mean was then evaluated. The limit on E_{QG} was then calculated from the ratio $\frac{\Delta T}{\Delta\langle E\rangle}$. The results coming from different flares were then averaged.
In order to smooth the fluctuations in the light curve and improve the evaluation of the peaking times a simple moving average was applied to the light curve. The subsets of data points averaged consisted of three points. As it is possible to notice from the graph, only two peaks are still well resolved. The peaking time was once again evaluated averaging the histogram in a symmetrical interval around each of the two maximum points. The value of E_{QG} was again calculated from the ratio $\frac{\Delta T}{\Delta\langle E\rangle}$. This procedure lead to a value of

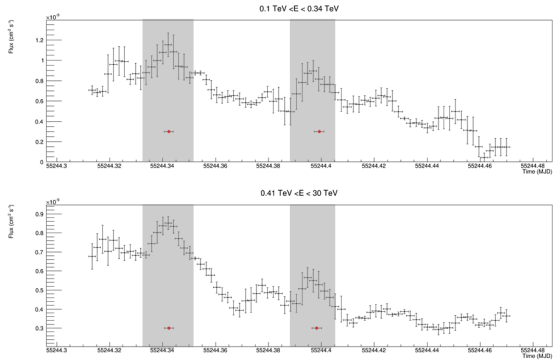

Figure 10: The graph represents the light curve after applying the moving average.

$E_{qg} = 2.5 \pm 2.9 \times 10^{12}$ TeV, corresponding to 95% confidence lower limit for E_{QG} equal to 1.1×10^{11} TeV.

4 Conclusions

This project studied the possibility of investigating Lorentz Invariance by means of VHE observations of flares in AGNs.
The simulation showed the difficulties of this analysis procedure, which are due mainly to the power-law spectrum of the source. In fact the presence of only a few photons in the higher energy bins and the necessity to make wide bins to have a significant population of photons in each of them affects the energy resolution.
These difficulties were encountered also during the analysis. The time resolution was also affected by the non-gaussian shape of the flare.
The value of E_{QG} measured is consistent with the values measured so far [7].

5 Acknowledgments

I really want to say thank you to all the people who helped me during the programme: Gernot, Anna, and all the people from the VERITAS gruoup I had the pleasure to spend my time with during this months. From each one of you I learned something, not only related to physics, and I am so grateful for this. Thank you Karl, for the time spent with and for us. I eventually wanted to say thank you to all the students who shared this experience with me, and made it so special.

References

[1] G. Amelino-Camelia, *Quantun Gravity Phenomenology*, Nuclear Physics B (Proc. Suppl.) **17**, 93-102 (1990)

[2] VERITAS web page, *VERITAS Specifications*, URL :http://veritas.sao.arizona.edu/about-veritas-mainmenu-81/veritas-specifications-mainmenu-111.

[3] http://tevcat.uchicago.edu/?mode=1& showsrc=75.

[4] S. E. Boggs, C. B. Wunderer, K.Hurley and W Coburn *Testing Lorentz invariance with GRB 021206*, The Astrophysical Journal, 611:L77-L80, 2004.

[5] W. Hofmann, *Comparison of Techniques to reconstruct VHE gamma-ray showers from multiple stereoscopic Cherenkov Images*, Astroparticle Physiscs (1999) 135-143.

[6] H. Prokoph,*Observations and modeling of the active galactic nucleus B2 1215+30 together with performance studies of the ground-based gamma-ray observatories VERITAS and CTA.* 2013

[7] A. Abramowski , *Search for Lorentz Invariance break with a likelyhood fit of the PKS 2155-304 flare data taken on MJD* , Astroparticle Physiscs (2011) 378-747.

[8] J. Ellis, N.E. Mavromatos *Probes of Lorentz Violations*, Astroparticle Physiscs 43 (2013) 50-55.

[9] Malcom S. Longair , *High Energy Astrophysics*, Cambridge University press (2011) .